Identification of Tyr504 as an Alternative Tyrosyl Radical Site in Human Prostaglandin H Synthase-2

ARTICLE *in* BIOCHEMISTRY · MARCH 2004

Impact Factor: 3.02 · DOI: 10.1021/bi035717o · Source: PubMed

6 AUTHORS, INCLUDING:

Corina Rogge
Museum of Fine Arts, Houston
20 PUBLICATIONS **508** CITATIONS
SEE PROFILE

Wen Liu
University of Texas Health Science Center at …
16 PUBLICATIONS **197** CITATIONS
SEE PROFILE

Gang Wu
University of Texas Health Science Center at …
30 PUBLICATIONS **462** CITATIONS
SEE PROFILE

Ah-Lim Tsai
University of Texas Health Science Center at …
142 PUBLICATIONS **4,604** CITATIONS
SEE PROFILE

Identification of Tyr504 as an Alternative Tyrosyl Radical Site in Human Prostaglandin H Synthase-2†

Corina E. Rogge,§ Wen Liu,§ Gang Wu,‡,§ Lee-Ho Wang, Richard J. Kulmacz, and Ah-Lim Tsai*

Department of Internal Medicine, University of Texas Health Science Center at Houston, Houston, Texas 77030

Received September 23, 2003; Revised Manuscript Received December 2, 2003

ABSTRACT: Hydroperoxides induce formation of a tyrosyl radical on Tyr385 in prostaglandin H synthase (PGHS). The Tyr385 radical initiates hydrogen abstraction from arachidonic acid, thereby mechanistically connecting the peroxidase and cyclooxygenase activities. In both PGHS isoforms the tyrosyl radical undergoes a time-dependent transition from a wide doublet to a wide singlet species; pretreatment with cyclooxygenase inhibitors results in a third type of signal, a narrow singlet [Tsai, A.-L.; Kulmacz, R. J. (2000) *Prost. Lipid Med. 62,* 231−254]. These transitions have been interpreted as resulting from Tyr385 ring rotation, but could also be due to radical migration from Tyr385 to another tyrosine residue. PATHWAYS analysis of PGHS crystal structures identified four tyrosine residues with favorable predicted electronic coupling: residues 148, 348, 404, and 504 (ovine PGHS-1 numbering). We expressed recombinant PGHS-2 proteins containing single Tyr → Phe mutations at the target residues, a quadruple mutant with all four tyrosines mutated, and a quintuple mutant, which also contains a Y385F mutation. All mutants bind heme and display appreciable peroxidase activity, and with the exception of the quintuple mutant, all retain cyclooxygenase activity, indicating that neither of the active sites is significantly perturbed. Reaction of the Y148F, Y348F, and Y404F mutants with EtOOH generates a wide singlet EPR signal similar to that of native PGHS-2. However, reaction of the Y504F and the quadruple mutants with peroxide yields persistent wide doublets, and the quintuple mutant is EPR silent. Nimesulide pretreatment of Y504F and the quadruple mutant results in an abnormally small amount of wide doublet signal, with no narrow singlet being formed. Therefore, the formation of an alternative tyrosine radical on Tyr504 probably accounts for the transition from a wide doublet to a wide singlet in native PGHS-2 and for formation of a narrow singlet in complexes of PGHS-2 with cyclooxygenase inhibitors.

The two isoforms of prostaglandin H synthase (PGHS), PGHS-1[1] and PGHS-2, catalyze the first committed steps in prostanoid biosynthesis, the conversion of arachidonic acid (AA) to prostaglandin G_2 via the cyclooxygenase activity and subsequent reduction of prostaglandin G_2 to prostaglandin H_2 through a classic peroxidase mechanism (*1*−*3*). The cyclooxygenase and peroxidase activities are mechanistically connected. The resting, ferric form of the enzyme reacts with hydroperoxides to form compound I (also termed intermediate I) containing a ferryl oxo porphyrin radical cation (*4*, *5*). This highly oxidized intermediate then undergoes an internal electron transfer, oxidizing Tyr385. This tyrosyl radical represents the junction of the two activities, as it is capable of abstracting the *pro-S* hydrogen from C13 of AA to initiate cyclooxygenase catalysis (*6*). The crystal structure of AA bound to CoPPIX-substituted ovine PGHS-1 shows that Tyr385 is located between the metalloporphyrin and the bound substrate, with the Tyr385 phenoxyl oxygen positioned close to C13 of AA (*7*).

Extensive EPR studies on both PGHS-1 and -2 have shown that the tyrosyl radical signal is not static; rather it undergoes several transitions based on reaction time, cyclooxygenase inhibitor binding, and self-inactivation (*8*). Upon reaction with hydroperoxides, both isoforms initially display a wide doublet (WD) signal that converts to a wide singlet (WS) within 50 s for PGHS-1 (WS1) but within 50 ms for PGHS-2 (WS2) (*9*). A similar transition of tyrosyl radical from WD to WS is found when PGHS-1 reacts normally with arachidonic acid (*11*). Further aging or self-inactivation of PGHS-1 results in the transition of the WS1 to a narrow singlet, NS1b (*10*−*12*). Complexes of either isoform with cyclooxygenase inhibitors, such as indomethacin or nimesulide, react with peroxide to form a second type of narrow singlet EPR signal (NS1a or NS2) (*13*, *14*). The NS1a signal seen in inhibitor-bound PGHS-1 is believed to be distinct from NS1b as NS1a displays more pronounced hyperfine features (*11*, *15*, *16*); this suggests that the tyrosine radical in NS1a resides on a tyrosine different from Tyr385. The existence of an alterna-

† This work was supported by United States Public Health Service Grants GM44911 (to A.-L.T.) and GM52170 (to R.J.K.) and postdoctoral fellowship DK61929 (to C.E.R.).

* To whom correspondence should be addressed at the Division of Hematology, University of Texas Health Science Center at Houston, P.O. Box 20708, Houston, TX 77225. E-mail: Ah-Lim.Tsai@uth.tmc.edu.

‡ Current address: Department of Biochemistry and Cell Biology, Rice University, Houston, TX 77005.

§ These authors contributed equally to this work.

[1] Abbreviations: PGHS-2, prostaglandin H synthase-2; PGHS-1, prostaglandin H synthase-1; EtOOH, ethyl hydrogen peroxide; WD, wide doublet tyrosyl radical; WS, wide singlet tyrosyl radical; NS, narrow singlet tyrosyl radical; EPR, electron paramagnetic resonance; ENDOR, electron nuclear double resonance spectroscopy; HF-EPR, high-field EPR; AA, arachidonic acid; PPHP, *trans*-5-phenyl-4-pentenyl-1-hydroperoxide; TMPD, *N*,*N*,*N*′,*N*′-tetramethyl-*p*-phenylenediamine; RFQ, rapid freeze quench; PPIX, protoporphyrin IX.

10.1021/bi035717o CCC: $27.50
Published on Web 01/24/2004

tive tyrosyl radical site is supported by studies of Y385F mutants of both PGHS-1 and -2. Reaction of these point mutants with peroxides results in formation of NS spectra, demonstrating that tyrosyl radicals at positions other than Tyr385 can be formed (*17*, *18*). Additional ENDOR and high-field EPR experiments with PGHS-1 have led to the following interpretations: The WD to NS1b transition can be accounted for by a rotation of the Tyr385 phenyl ring bearing the unpaired electron, thereby altering the interactions of the α-carbon hydrogens with the p_z orbital of C1 (*19*). The WS1 signal can be simulated by arithmetic combinations of the WD1 and NS1b signals, suggesting that WS1 is not a distinct species but rather represents a mixture of signals from two species (*8*, *12*, *15*). Therefore, the tyrosine radical in PGHS-1 may both undergo rotation (WD1 → NS1b) and migration (WD1 → NS1a). Although the EPR characteristics of the PGHS-2 radicals are less well studied, the WD → WS transition can be accounted for by either rotation of the aromatic ring of Tyr385 or a combination of WD and NS radicals as seen in PGHS-1, again suggesting that either ring rotation alone or both ring rotation and electron migration might occur (*9*).

The multiple EPR signals observed during the peroxidase reaction cycle of PGHS can complicate data interpretation, especially as the signals all have similar field positions and power saturation profiles (*13*, *17*). To better understand the observed EPR transitions, we undertook to determine if the WD → WS transition in native PGHS-2 and the formation of an NS in inhibitor-treated PGHS-2 could be accounted for by formation of a radical on an alternative tyrosine residue or by ring rotation at Tyr385. Four tyrosines, Tyr148, Tyr348, Tyr404, and Tyr504 (ovine PGHS-1 numbering), in the vicinity of both the heme and Tyr385 were identified as candidate alternative radical sites and mutated to phenylalanine. The results suggest that formation of a second radical at Tyr504 accounts for both the WD → WS transition in native PGHS-2 and the NS formation in both inhibitor-treated PGHS-2 and the Y385F mutant.

EXPERIMENTAL PROCEDURES

Materials. AA was from NuChek Preps (Elysian, MN); EtOOH was purchased as a 5% aqueous solution from Polysciences (Warrington, PA). PPHP and nimesulide were from Cayman Chemical (Ann Arbor, MI), and Tween-20 and *n*-octyl β-D-glucopyranoside were from Anatrace (Maumee, OH). All other reagents were obtained from Sigma-Aldrich.

Electron-Transfer Pathways Analysis. Calculations were performed using HARLEM, the PATHWAYS analysis program, of Beratan and Onuchic (*20*, *21*). In this algorithm, the overall coupling efficiency of a given path is the product of individual coupling factors for through-covalent-bond, through-hydrogen-bond, and through-space decay along that path. Through-covalent-bond decay, ϵ_C, is set to 0.6, and through-hydrogen-bond decay, ϵ_H, is $0.6^2e^{-1.7(R-2.8)}$, where R is the H-atom to H-bond-accepting heavy atom distance. This correction allows for exponential decay across longer hydrogen bonds. Through-space decay, ϵ_S, equal to $^1/_2(0.6e^{-1.7(R-1.4)})$, varies exponentially with the distance of the jump, R. The optimal electron-transfer pathway was determined between each of the 27 tyrosines (as a residue) and heme (as a group) and between each tyrosine (as a residue) and Tyr385 (as a residue), using crystallographic coordinate sets (PDB) for mouse PGHS-2 (5COX) (*22*) and ovine PGHS-1 (1DIY) (*7*).

Construction of PGHS-2 Plasmids with Single Tyrosine Point Mutations. The QuikChange site-directed mutagenesis kit (Stratagene, CA) was used with a template containing the human PGHS-2 cDNA inserted into the pSG5 plasmid (*23*) and the following primer pairs (base changes are underlined):

```
Y148F-F 5′-CTCTAACCTCTCCTATTTTACTAGAGCCCTTCC-3′

Y148F-R 5′-GGAAGGGCTCTAGTAAAATAGGAGAGGTTAGAG-3′

Y348F-F 5′-GTGATTGAAGATTTTGTGCAACACTTGAGTGGC-3′

Y348F-R 5′-GCCACTCAAGTGTTGCACAAAATCTTCAATCAC-3′

Y385-F 5′-CTGAATTTAACACCCTCTTTCACTGGCATCCCCTTC-3′

Y385-R 5′-GAAGGGGATGCCAGTGAAAGAGGGTGTTAAATTCAG-3′

Y404F-F 5′-CATGACCAGAAATACAACTTTCAACAGTTTATCTAC-3′

Y404F-R 5′-GTAGATAAACTGTTGAAAGTTGTATTTCTGGTCATG-3′

Y504F-F 5′-CGATGCTGTGGAGCTGTTTCCTGCCCTTCTGGTAG-3′

Y504F-R 5′-CTACCAGAAGGGCAGGAAACAGCTCCACAGCATCG-3′
```

The cDNAs containing the desired mutations were inserted into the pVL1393 vector (PharMingen, CA). The integrity of the resulting transfer vector constructs was verified by restriction enzyme digestion and DNA sequencing.

Construction of PGHS-2 Plasmids with Multiple Site Mutations. The QuikChange site-directed mutagenesis kit and the QuikChange multi-site-directed mutagenesis kit (Stratagene, CA) were used for construction of the hPGHS2 quadruple mutant (Y148F/Y348F/Y404F/Y504F) and the quintuple mutant (Y148F/Y348F/Y385F/Y404F/Y504F). The 5′-phosphorylated primer sequences containing the mutation (base changes are underlined) were

```
Y148F 5′-CTCTAACCTCTCCTATTTTACTAGAGCCCTTCC-3′

Y348F 5′-GTGATTGAAGATTTTGTGCAACACTTGAGTGGC-3′

Y385F 5′-CTGAATTTAACACCCTCTTTCACTGGCATCCC-3′

Y404F 5′-CATGACCAGAAATACAACTTTCAACAGTTTATCTAC-3′

Y504F 5′-GATGCTGTGGAGCTGTTTCCTGCCCTTCTGGTAG-3′
```

Mutagenesis reactions were carried out using equal amounts of the five 5′-phosphorylated primers, and the reaction product was used to transform *E. coli* XL-10 competent cells. One clone containing a double mutation (Y348F/Y504F) was used as template DNA with the Y148F and Y404F sense and antisense primers (see above) to construct the desired quadruple mutant. Another clone containing a quadruple mutant (Y148F/Y348F/Y385F/Y504F) was used as template DNA with the Y404F sense and antisense primers (see above) to construct the quintuple mutant. The cDNAs containing the desired quadruple and quintuple mutations were inserted into the pVL1393 vector,

and the integrity of the resulting transfer vector constructs was confirmed by restriction enzyme digestion and DNA sequencing.

Baculovirus Generation, and Expression and Purification of Recombinant Proteins. Procedures for generation, amplification, and titer determination of recombinant baculovirus containing cDNA for the desired PGHS-2 proteins have been described (*24*).

For expression of the recombinant proteins, Sf9 cells were grown in suspension to $\sim 1 \times 10^6$ cells/mL and infected with the desired recombinant virus at ~10 plaque-forming units/cell. Cells were harvested 3 days later and stored at −80 °C until purification. Detergent-solubilized preparations of the recombinant PGHS-2 proteins were prepared as described elsewhere (*24*). For RFQ-EPR experiments with the Y504F and quadruple mutants, the detergent-solubilized preparations were further purified by chromatography on an AcA34 gel filtration column. Holoenzymes were reconstituted with heme as previously described (*9*).

Protein Characterization. The concentrations of recombinant PGHS-2 apoenzymes were determined by dot blot (*24*). PGHS-2 holoenzyme concentrations were determined on the basis of heme content as calculated from the absorbance at 406 nm (165 mM^{-1} cm^{-1}). PGHS-2 mutants were analyzed by electrophoresis under denaturing conditions on 10% polyacrylamide gels and visualized either by Coomassie blue staining or by transfer to nitrocellulose membranes and subsequent immunoblot processing using the antibody against PGHS-2 and the BioRad Opti-4CN kit.

Cyclooxygenase Activity. Oxygen uptake was assayed polarographically at 30 °C as described previously (*25*). One unit of cyclooxygenase activity has an optimal velocity of 1 nmol of O_2/min. Cyclooxygenase K_M values were determined by measuring the activity with 1−60 μM AA and fitting the values to the Michaelis−Menten equation using Kaleidagraph software (Synergy Software). Cyclooxygenase self-inactivation rates were calculated by dividing the optimal velocity (nmol of O_2/min) by the reaction extent at complete self-inactivation (nmol of O_2 consumed) (*26*).

Peroxidase Activity. Measurements were performed at room temperature using a Bio-SEQUENTIAL DX-18MV stopped flow instrument (Applied Photophysics, Leatherhead, U.K.). Peroxidase activity was measured by monitoring TMPD oxidation at 611 nm during the reaction of enzyme with H_2O_2. One syringe contained 1.6 mM H_2O_2, the other 20 mM TMPD and enzyme in 100 mM Tris−HCl, pH 8.5. Specific activity values were calculated using an extinction coefficient for oxidized TMPD of 13.5 mM^{-1} cm^{-1}, assuming 2 mol of TMPD oxidized/mol of peroxide reduced, and were normalized to the amount of recombinant enzyme. Final values are given in units per microgram of recombinant protein, where 1 unit is 1 nmol of peroxide reduced/min. Peroxidase K_M values were determined by measuring guaiacol oxidation in reactions with 2−150 μM PPHP. Guaiacol oxidation (10 mM final concentration) was monitored at 436 nm (3.33×10^4 M^{-1} cm^{-1}). Velocity vs substrate concentration data were fitted to the Michaelis−Menten equation using SigmaPlot 8.0 software (SPSS Inc).

EPR and RFQ-EPR Experiments. Initial EPR analysis of tyrosyl radicals generated by the PGHS-2 mutants was done by hand-mixing each detergent-solubilized PGHS-2 preparation with 15 equiv of EtOOH on ice for 10 s and then freezing the sample in an acetone/CO_2 bath. For complexes of PGHS-2 with nimesulide, the enzymes were incubated with a 2-fold molar excess of nimesulide at room temperature for 0.5−1 h before reacting with EtOOH. Cyclooxygenase activity after nimesulide treatment was <20% that of the untreated activity.

RFQ experiments were performed using an Update Instruments (Madison, WI) System 1000 chemical/freeze quench apparatus with a model 1019 syringe ram, a model 715 ram controller, and a 0.008 in. nozzle. The ram velocity was 2.0 cm/s, and the dead time was 4−5 ms. An isopentane bath at 125−130 K was used to chill the packing assembly before sample collection and during pressure filtration packing (*27*).

EPR spectra of samples were recorded on a Bruker EMX spectrometer at a modulation amplitude of 2.00 G, modulation frequency of 100 kHz, time constant of 327 ms, microwave power of 1 mW, and temperature of 113 K. Radical concentrations were determined by double integration of the EPR signals with reference to a copper standard (*11*); calculations for RFQ-EPR samples used a packing correction factor of 0.45.

RESULTS

Electron-Transfer Analyses. Visual examination of crystallographic data for PGHS-1 and PGHS-2 (PDB codes 1DIY and 1CQE) located three tyrosine residues (Tyr348, Tyr148, and Tyr404) that are within 7 Å of the heme and that could be sites for alternative tyrosyl radical formation. PATHWAYS analysis of mouse PGHS-2 and ovine PGHS-1 identified an additional residue, Tyr504, as a candidate for mutational analysis; indeed, Tyr504 showed the second highest predicted electron coupling efficiency (Table 1). The positions of the candidate tyrosines relative to the heme and Tyr385 are shown in Figure 1. Tyr148, Tyr348, and Tyr504 are strictly conserved in mammalian PGHS-1 and PGHS-2, whereas Tyr404 is conservatively substituted with phenylalanine in some mammalian PGHS-1 and -2 sequences. Table 1 shows the calculated paths, distances, and predicted electron-transfer coupling factors from each of these tyrosines to Tyr385 and to the heme cofactor. The order of predicted coupling efficiency to Tyr385 is Tyr348 > Tyr504 > Tyr404 > Tyr148, while that to the heme is Tyr148 > Tyr504 > Tyr348 > Tyr404.

Electrophoretic Analysis of Native and Mutant PGHS-2 Proteins. Polyacrylamide gel electrophoresis and subsequent visualization by immunoblot of the detergent-solubilized fractions revealed a major band at ~73 kDa for native PGHS-2 and each of the mutants (data not shown). This indicates that all mutants are overexpressed in the baculovirus system as detergent-soluble full-length proteins analogous to native PGHS-2.

Cyclooxygenase Activity. To assess the effects of the mutations on cyclooxygenase functional integrity, we determined the specific activity, the K_M for arachidonic acid, and the inactivation rate for each mutant protein (Table 2). All mutants except for Y385F and the quintuple mutant have cyclooxygenase activity comparable to that of the native enzyme. The Y348F and the quadruple mutant have specific activities approximately half that of native PGHS-2, perhaps due to loss of the Tyr348 hydrogen bond to the Tyr385 phenoxyl oxygen. All mutants have K_M values within a factor

Table 1: Predicted Optimal Electron-Transfer Pathways from Selected Tyrosine Residues to Tyr385 and to Heme in Mouse PGHS-2 (PDB Code 5COX) (*22*)[a]

donor/ acceptor	optimal pathway	pathway distance (Å)	predicted coupling
	Tyr/Heme		
Y385	Y385 ⇒ heme	3.1	3.2×10^{-2}
Y148	Y148 ⇒ heme	4.2	5.2×10^{-3}
Y504	Y504 ⇒ H388 ⟶ heme	8.4	4.0×10^{-4}
Y348	Y348 ⇒ Y385 ⇒ heme	6.1	1.5×10^{-4}
Y404[b]	Y404 → L408 ⇒ heme	10.0	4.6×10^{-5}
	Tyr/Tyr385		
Y348	Y348 ⇒ Y385	2.6	7.3×10^{-2}
Y504	Y504 ⇒ H386 ⟶ Y385	6.6	2.1×10^{-3}
Y404[b]	Y404 → L408 ⇒ Y385	5.1	3.5×10^{-4}
Y148	Y148 ⟶ T149 → S379 → T383 → H386 ⟶ Y385	9.8	1.4×10^{-4}

[a] A double arrow (⟶) indicates a through-bond coupling; hydrogen bonds and through-space jumps are indicated by → and ⇒, respectively. [b] Calculated using coordinates (PDB) for ovine PGHS-1 (1DIY) (*7*).

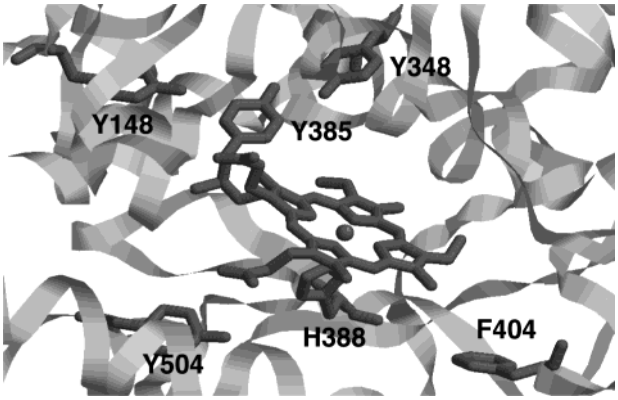

FIGURE 1: Mouse PGHS-2 crystallographic structure (*22*) showing the relative positions of residues selected for mutation. Residue 404 is a phenylalanine in mouse PGHS-2 but a tyrosine in the human enzyme.

of 2 of the native enzyme, indicating minimal disruption of the cyclooxygenase active site structure. Cyclooxygenase self-inactivation occurs in both PGHS isoforms, and is believed to be a radical-driven process. Removal of alternate radical sites or electron-transfer paths thus could conceivably alter inactivation rates. Modest increases in inactivation rates are seen for Y404F (2.3-fold) and the quadruple mutant (2.3-fold), indicating that only the identity of residue 404 has a major influence on cyclooxygenase self-inactivation.

Peroxidase Kinetics. Native PGHS-2 has a peroxidase specific activity of 14.1 units/μg, similar to those of Y148F, Y348F, Y404F, and the quadruple mutant (Table 2). The quintuple mutant has about half of the native peroxidase and cyclooxygenase activities, suggesting that the multiple mutations have a cumulative effect on the overall enzyme activity. Interestingly, the Y504F and Y385F mutants have about twice the peroxidase activity of native PGHS-2. These two mutants, as well as the quadruple mutant, also show severalfold increases in the K_M value for an organic peroxide, PPHP (Table 2). On the other hand, Y148F and Y404F have K_M values of 15% and 45% that of the wild type, respectively. These changes in specific activity and K_M for peroxide may be due to changes in the efficiency of reaction with cosubstrate. The peroxidase cycle is a bisubstrate sequential reaction, so the K_M and V_{max} values for one substrate are proportional to the rate of reaction with the other substrate. Therefore, a higher cosubstrate concentration, or a faster rate constant for reaction with cosubstrate, raises the observed V_{max} and the K_M for peroxide; conversely, a decreased rate of reaction will decrease the observed V_{max} and K_M values (*28*).

Tyrosyl Radical EPR Spectra of Mutant and Native PGHS-2. Addition of EtOOH to native PGHS-2 and the mutants results in formation of tyrosyl radicals (Figure 2). As observed previously, manual mixing of native PGHS-2 with peroxide produces a wide singlet of ~29 G (peak to trough) centered at $g = 2.004$, and the Y385F mutant forms a narrow singlet of ~21 G line width (*18*, *29*). The radicals formed by the Y148F, Y348F, and Y404F mutants have EPR spectra very similar to that of the native enzyme, wide singlets ~28−29 G in width centered at $g = 2.003-2.004$. In contrast, the reaction of the Y504F and quadruple mutants with peroxide results in very different EPR spectra, wide doublets centered at $g = 2.003$, with ~19 G hyperfine splitting, and ~30 G in width. The tyrosyl radicals of the Y504F and quadruple mutants have $P_{1/2}$ values of 1.0 mW (data not shown), which are similar to the previously reported value for native PGHS-2 (*30*). The quintuple mutant has virtually no signal in the $g = 2$ region, indicating that treatment with EtOOH does not form organic radicals. The intensities of the tyrosyl radical signals observed in the present samples (0.02−0.06, [spin]/[heme]) are significantly lower than those seen previously using purified native PGHS-2 (*14*). This low yield of signal may be due to the phenol included as a stabilizer, although previous studies have shown that the phenol concentration used (50 μM) has little effect on tyrosyl radical formation rates or intensities (*9*). Additional purification of the recombinant PGHS-2 proteins by gel filtration chromatography on AcA34 does not significantly alter the intensities of the tyrosyl radicals (data not shown).

Tyrosyl Radical Kinetics in Y504F and the Quadruple Mutant. The kinetics of the Y504F and quadruple mutant tyrosyl radical signals were characterized by RFQ-EPR on samples purified by gel filtration chromatography. The results, shown in Figures 3 and 4, include data obtained with two separate preparations of each of the mutants. When the Y504F mutant is reacted with 15 equiv of EtOOH at room temperature, the wide doublet signal rapidly forms within the 4 ms dead time and plateaus at an intensity of ~0.11 ([spin]/[heme]) for ~750 ms before undergoing a slow decay in intensity ($k = 0.1\ s^{-1}$) (Figure 3). As shown in the bottom panel of Figure 3, the later decrease in intensity is not accompanied by any change in line shape. With the

Table 2: Cyclooxygenase and Peroxidase Kinetic Parameters of Detergent-Solubilized Native and Mutant PGHS-2 Proteins[a]

	cyclooxygenase			peroxidase	
PGHS-2 construct	specific activity (u/μg)	K_M (μM AA)	k_{inact} (min^{-1})	specific activity (u/μg)	K_M (μM PPHP)
native	5.8 ± 0.1	2.1 ± 0.4[b]	2.3 ± 0.1	14.1 ± 0.3	138 ± 42
Y148F	5.8 ± 0.3	3.2 ± 0.7	3.0 ± 0.0	9.9 ± 0.2	20 ± 8
Y348F	2.7 ± 0.1	3.8 ± 0.7	2.7 ± 0.3	15.0 ± 0.6	72 ± 22
Y385F		not detected		26.1 ± 0.6	339 ±165
Y404F	4.7 ± 0.1	3.6 ± 0.4	5.3 ± 0.4	11.1 ± 0.3	61 ± 30
Y504F	3.9 ± 0.0	4.2 ± 0.4	2.2 ± 0.1	34.0 ± 0.9	437 ± 79
quad[c]	2.3 ± 0.1	4.3 ± 1.0	5.4 ± 0.4	10.6 ± 0.2	370 ± 130
quint[d]		not detected		6.4 ± 0.3	103 ± 42

[a] Values represent averages of at least three assays' with standard deviation indicated. [b] Value taken from ref *24*. [c] Quadruple mutant (Y148F/Y348F/Y404F/Y504F). [d] Quintuple mutant (Y148F/Y348F/Y385F/Y404F/Y504F).

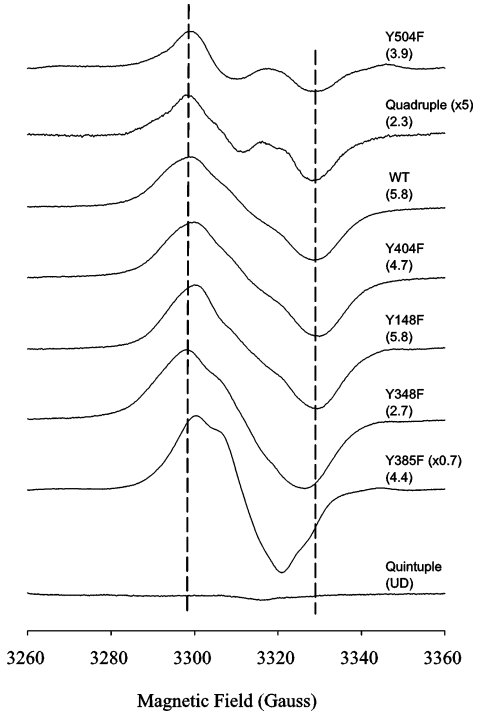

FIGURE 2: EPR spectra of tyrosyl radicals formed upon reaction of native and mutant PGHS-2 with EtOOH. The enzymes in 100 mM KPi, pH 7.2, 50 μM phenol, 0.04% octyl glucoside were reacted on ice with 15 equiv of EtOOH for ~10 s. The values in parentheses represent the radical intensities ([spin]/[heme]) × 100; UD = undetermined.

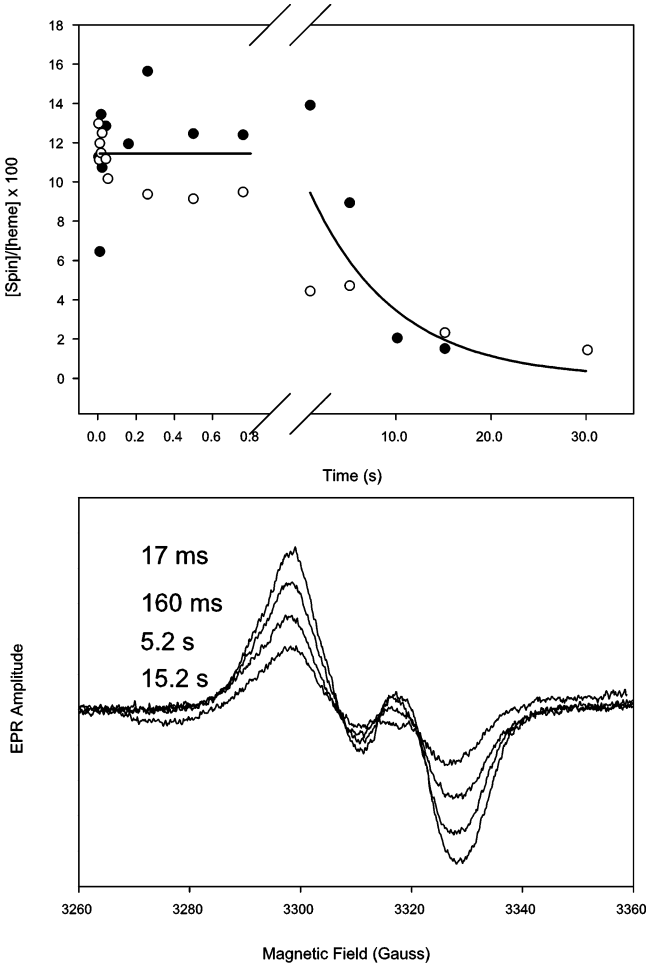

FIGURE 3: Tyrosyl radical kinetics during reaction of the Y504F mutant with EtOOH. The Y504F mutant (48 μM heme) in 100 mM KPi, pH 7.2, 50 μM phenol, 0.04% octyl glucoside, 10% glycerol was reacted at room temperature with 15 equiv of EtOOH. Top panel: time course of tyrosyl radical intensities as determined by double integration of the EPR signals. The solid and open circles represent data obtained from two different enzyme preparations. Bottom panel: EPR spectra acquired for representative Y504F reaction samples freeze-trapped at the indicated times.

quadruple mutant, the wide doublet tyrosyl radical forms more slowly (k > 200 s^{-1}) (Figure 4) than that of the Y504F mutant. This rate difference may reflect the different glycerol concentrations used in the two samples (5% and 10% final concentration for Y504F and the quadruple mutant, respectively). The radical intensity for the quadruple mutant plateaus at ~0.11 ([spin]/[heme]) before decaying, at 0.3 s^{-1}, again without a change in line shape. These results indicate that only one tyrosyl radical species, a wide doublet probably located on Tyr385, forms during reaction of either Y504F or the quadruple mutant with peroxide. Mutation of Tyr504 thus prevents the transition from an initial wide doublet to a later wide singlet, as seen in native PGHS-2 (*9*). This indicates that the transition to wide singlet involves formation of an alternate tyrosyl radical at Tyr504.

EPR of Nimesulide-Treated PGHS-2 Isoforms. Each of the recombinant proteins was incubated with a 2-fold excess of nimesulide to form the cyclooxygenase inhibitor complex before reaction with EtOOH. The tyrosyl radical spectra obtained are shown in Figure 5. As expected, the inhibitor complex of the native PGHS-2 gives an NS EPR signal (~21 G wide) centered at g = 2.003. The signals from the inhibitor complexes of Y148F, Y348F, Y385F, and Y404F mutants

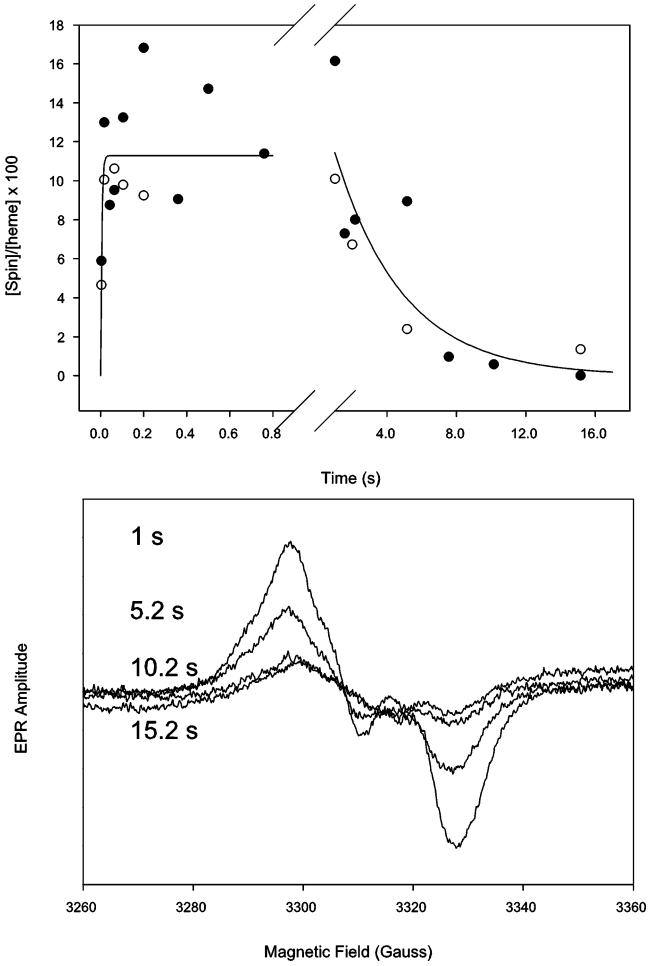

FIGURE 4: Tyrosyl radical kinetics for reaction of the quadruple mutant with EtOOH. The quadruple mutant (37 μM heme) in 100 mM KPi, pH 7.2, 50 μM phenol, 0.04% octyl glucoside, 20% glycerol was reacted at room temperature with 15 equiv of EtOOH. Top panel: time course of tyrosyl radical intensities as determined by double integration of the EPR signals. The solid and open circles represent data obtained from two different enzyme preparations. Bottom panel: EPR spectra acquired for representative samples freeze-trapped at the indicated times.

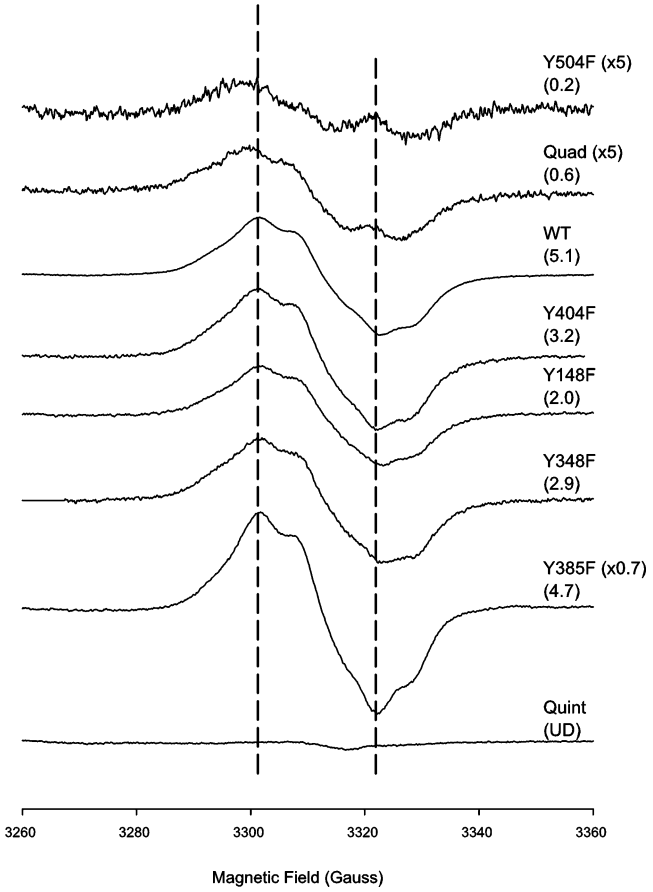

FIGURE 5: EPR spectra of tyrosyl radicals formed by nimesulide-treated PGHS-2 proteins upon reaction with EtOOH. Each protein was dissolved in 100 mM KPi, pH 7.2, 50 μM phenol, 0.04% octyl glucoside, pretreated with 2 equiv of nimesulide until the residual cyclooxygenase activity was <20% of the original value, and then reacted on ice with 15 equiv of EtOOH for ~10 s. The values in parentheses represent the radical intensities ([spin]/[heme]) × 100; UD = undetermined.

all are narrow singlets analogous to that of the native enzyme, whereas the inhibitor complex of the quintuple mutant yields no discernible radical upon reaction with peroxide. However, the Y504F and the quadruple mutants give very small amounts of a radical resembling the wide doublet (signal intensities of 0.002 and 0.006 compared to 0.02−0.051 ([spin]/[heme]) for the other proteins). Nimesulide binding was confirmed by observation of cyclooxygenase inhibition for each of the proteins, so the EPR results indicate that mutation of Tyr504 prevents formation of the NS radical. This identifies Tyr504 as the site of the tyrosyl radical formed in PGHS-2 complexed with cyclooxygenase inhibitors.

DISCUSSION

Tyrosyl radicals have emerged as important catalytic components in many proteins, including class I ribonucleotide reductases, bovine liver catalase, photosystem II, galactose oxidase, and the catalase-peroxidase KatG (*31*−*36*). Transient tyrosyl radicals have also been seen during catalysis in taurine/α-ketoglutarate dioxygenase and in hemoglobin and myoglobin after treatment with H_2O_2 (*37*, *38*). However, none of these tyrosyl radicals have the same catalytic role as the tyrosyl radical in PGHS, namely, abstraction of a hydrogen atom from an organic substrate. Also unlike the previously mentioned enzymes, the tyrosyl radicals in PGHS-1 and -2 undergo spectroscopic transitions from wide doublet to wide singlet and narrow singlet species. One current hypothesis to account for these transitions in PGHS-1 is that the initial wide doublet (WD1) species formed with the radical on Tyr385 converts via phenyl ring rotation to a narrow singlet (NS1b), the same species seen upon self-inactivation (*6*, *16*). Arithmetic combination of WD1 and the NS1b signals produces the observed wide singlet (WS1), so the overall observed transition is WD1 → [WS1] → NS1b. Binding of cyclooxygenase inhibitors to PGHS-1 before reaction with peroxides leads to the formation of a second, distinct narrow singlet tyrosyl radical (NS1a) that is believed to reside upon a residue other than Tyr385. Only three types of tyrosyl radical spectra have been seen in PGHS-2: a transient wide doublet (WD2) that very quickly converts to a wide singlet (WS2), and a narrow singlet (NS2) observed when cyclooxygenase inhibitors are bound (*9*).

The present results suggest that the WD2 to WS2 transition in PGHS-2 results from tyrosyl radical migration from Tyr385 to Tyr504 rather than from tyrosyl ring rotation, as the Y504F mutant shows a persistent wide doublet that does

not convert to a wide singlet even after long reaction times. Initial formation of the Y504F WD2 is complete within 4 ms, even faster than WD2 formation in native PGHS-2, which has a rate of 150 s^{-1} and reaches a plateau at 50 ms (*9*). The fast rate of WD2 formation and the high cyclooxygenase activity of Y504F suggest that the WD2 radical is kinetically competent to initiate cyclooxygenase catalysis. The quadruple mutant behaves similarly to Y504F, although its decreased activity and higher cyclooxygenase self-inactivation rate render it less attractive for mechanistic studies.

Complexation of Y504F and the quadruple mutant with nimesulide prior to reaction with EtOOH results in minimal formation of a WD2 signal and no formation of a narrow singlet (Figure 5). In contrast, the Y148F, Y348F, and Y404F mutants all exhibit the same NS as the native PGHS-2 inhibitor complex. Tyr504, therefore, is clearly critical for NS2 formation. The simplest explanation for these results is that most radical formation at Tyr385 is blocked in the nimesulide-treated samples and the radical instead forms on Tyr504; if this residue is mutated, no tyrosine radical forms. If radical migration from Tyr385 to Tyr504 were occurring in inhibitor-treated enzyme, a WD signal approximately equal in intensity to the NS of other mutants would be seen in Y504F, which is not the case. An alternative explanation, that the Tyr385 radical forms initially in Y504F but dissipates faster than the time scale of the experiment, is unlikely given the observed persistence of all tyrosyl radical signals observed so far. Previous RFQ-EPR studies of the tyrosyl radical in nimesulide-treated PGHS-2 showed that the NS2 species formed within 5 ms (*9*), also supporting initial radical formation on Tyr504. These results suggest that nimesulide binding alters the site of radical formation from Tyr385 to Tyr504, perhaps by changing the relative redox potentials of these two residues. The electronic coupling between Tyr385 or Tyr504 and the heme may also change as the result of structural perturbation upon inhibitor binding, although such an alteration is not apparent in PGHS-2 crystallographic structures with and without inhibitor bound.

The different line shapes arising from radicals on Tyr504 (WS2 in native PGHS-2 and NS2 in the inhibitor complex) may be due either to two distinct conformations of Tyr504 or, as in PGHS-1, to one conformation (NS2) that combines with the Tyr385 WD2 to give the observed WS2. If the WS2 and NS2 signals represent different conformations of a Tyr504 radical, the conformational change could be triggered by inhibitor binding. However, inspection of crystal structures of PGHS-2 with and without bound inhibitors (*41*) reveals no obvious difference in the Tyr504 environment or ring orientation. In addition the Y385F mutant gives only an NS signal, even in the absence of inhibitor (Figure 2). If the WS2 arises from arithmetic combination of the Tyr385 WD2 and a Tyr504 NS2, the RFQ-EPR data suggest that initial radical formation in native PGHS-2 occurs on Tyr385 but then rapidly equilibrates to a Tyr385/Tyr504 radical mixture. Further high-field EPR and ENDOR studies will be required to elucidate the precise nature of the WS2 and NS2 radicals. On the basis of the present data, it seems most likely that the WD2 → WS2 transition in PGHS-2 arises from partial or complete radical migration from Tyr385 to Tyr504 and that binding of cyclooxygenase inhibitors diverts radical formation to Tyr504, resulting in the NS2 signal. This conclusion has some mechanistic significance as it focuses on a Tyr385 wide doublet radical as the direct oxidant of fatty acid in PGHS-2 cyclooxygenase catalysis.

The lack of any radical EPR signals upon reaction of the quintuple mutant with peroxide, and the similarity of the EPR signals from native PGHS-2 and the Y148F, Y348F, and Y404F mutants, shows that tyrosyl radicals are not formed on residues other than Tyr385 and Tyr504 and that the extent of radical migration is limited to Tyr504 alone. Y385F gives only a narrow singlet, Y504F shows only a wide doublet, and all other single point mutants show spectra similar to that of the native enzyme. If radical migration to other tyrosines besides Tyr504 could occur, further signal transitions in Y504F would be expected as new tyrosyl radicals, with different environments and dihedral angles, were formed. The exclusive formation of an alternative radical on Tyr504 is somewhat surprising when the PATHWAYS analysis results in Table 2 are considered. Tyr148 is predicted to be more efficiently coupled to the heme than is Tyr504, and Tyr348 is predicted to be more efficiently coupled to Tyr385 than Tyr504, yet neither Tyr148 nor Tyr348 is susceptible to radical formation during the PGHS-2 reaction with peroxide. However, it should be noted that the coupling between the heme and Tyr504 was calculated without the crystallographic water molecule found in the refined structure of ovine PGHS-1 (*39*). The presence of such a water molecule would eliminate the through-space jump and allow coupling of the heme and Tyr504 through hydrogen bonds, which would increase the predicted coupling efficiency.

Blocking formation of the alternative tyrosyl radical at Tyr504 has little effect on cyclooxygenase activity, as evidenced by the similar cyclooxygenase specific activities, K_M values for AA, and product ratios of native and Y504F PGHS-2 (Table 2 and ref *40*). Further, previous studies indicated that the PGHS-2 WS2 is kinetically competent to react with AA in cyclooxygenase catalysis (*18*). Taken together, these data indicate that the tyrosyl radicals at Tyr385 and Tyr504 are in equilibrium. If they were not, formation of the Tyr504 radical would be expected to decrease cyclooxygenase catalysis, as a Tyr504 radical is not located near AA. An estimate of the Tyr385 and Tyr504 radical proportions in the native enzyme indicates how dramatically cyclooxygenase catalysis would be impacted in the absence of equilibration. In PGHS-2 a WD2/NS2 ratio of 30/70 best simulates the WS spectrum.[2] If radical migration to Tyr504 were irreversible, then less than half of the radical present in the WS of native PGHS-2 would be capable of cyclooxygenase activity. However, native PGHS-2, which can form the Tyr504 radical, has a higher cyclooxygenase specific activity than the Y504F mutant, which can only form a radical on Tyr385. Also, previous single turnover studies using native PGHS-2 show 80−90% conversion of the WS2 tyrosyl radical to the arachidonyl radical (*18*). Therefore, electron transfer between Tyr385 and Tyr504 is likely to be reversible, with the Tyr504 radical representing a reservoir of oxidant for cyclooxygenase catalysis.

Cyclooxygenase activity was retained in the Y504F mutant of murine PGHS-2 (*40*). However, in PGHS-1 the Y504F

[2] Rogge, C. E., Kulmacz, R. J., and Tsai, A.-L., unpublished results.

and Y504Q mutants were reported to lack both cyclooxygenase and peroxidase activities, whereas the Y504A mutant retains considerable amounts of both activities (*39*). This suggests that the alternative tyrosyl radical site is not essential for catalytic activity in either isoform, but that the structure of the residue at 504 can have isoform-specific effects. The PGHS-1 tyrosyl radical undergoes a transition from a WD to a WS during reaction with arachidonate (*11*), raising the possibility that radical migration has some connection to cyclooxygenase catalysis. Further studies are necessary to determine whether Tyr504 is also an alternative radical site in PGHS-1 and to define the mechanistic implications of any radical migration.

Irreversible self-inactivation is observed for both PGHS isoforms during cyclooxygenase catalysis (*42*, *43*). The self-inactivation process is believed to involve oxidative damage to the protein, although the exact mode and mechanism have not been defined. The tyrosyl radical in intermediate II has been implicated in PGHS-1 peroxidase self-inactivation (*44*), and both Tyr385 and Tyr504 radicals might plausibly participate. The observation of similar cyclooxygenase self-inactivation rates in native PGHS-2 (with both Tyr385 and Tyr504 radicals) and the Y504F mutant (with only the Tyr385 radical) (Table 2) suggests that the radical migration to Tyr504 does not significantly affect the overall process of cyclooxygenase self-inactivation.

The identification of Tyr504 as the alternative radical in PGHS-2 and the apparent reversibility of electron transfer from Tyr385 to Tyr504 are somewhat reminiscent of the situation in ribonucleotide reductase R2 (*45*). In this enzyme, a tyrosyl radical generated by the diiron cofactor in one subunit serves as a "pilot light" for catalytic events in a second subunit. The electron is proposed to be reversibly transferred over a distance of 35−40 Å, generating a transient thiyl radical responsible for deoxygenation of ribonucleic acids (*46*−*48*). In PGHS-2, Tyr385 is the site of the initial tyrosyl radical, but this apparently quickly equilibrates with a radical at Tyr504, which might serve as a pilot light in this enzyme, transferring back to Tyr385 to react with substrate. However, unlike Tyr122 in ribonucleotide reductase R2, Tyr504 is not essential to PGHS-2 catalysis, as Tyr504F is fully active (Table 2), so any mechanistic advantage of the radical equilibration between Tyr385 and Tyr504 remains to be determined. It may be that the Tyr385/Tyr504 radicals in PGHS-2 are more similar to the Y_Z/Y_D radical pair in photosystem II, where Y_Z is essential for electron transfer from the tetranuclear manganese water-oxidizing complex to P_{680} and Y_D has no defined function, although the radical is also coupled to the water-oxidizing complex (*49*). Tyr504 and Y_D may represent evolutionary holdovers, but given the high conservation of each, it is likely that they have important functions yet to be determined.

In summary, we have identified Tyr504 as the alternative radical site in PGHS-2 responsible for the WD → WS transition and NS formation. The conservative Y504F mutation does not greatly affect either cyclooxygenase or peroxidase activity, indicating that the Tyr504 radical is not essential for catalysis. The generation of a single tyrosyl radical species on Tyr385 and the high catalytic activity of the Y504F mutant make it very attractive for further mechanistic studies. Given the similarities between PGHS-1 and -2, Tyr504 may also be an alternative tyrosyl radical in PGHS-1.

ACKNOWLEDGMENT

We thank Drs. David Beratan and Igor Kurnikov at Duke University for providing the HARLEM program for PATHWAYS analysis.

REFERENCES

1. Smith, W. L., and Dewitt, D. L. (1996) Prostaglandin endoperoxide H synthases-1 and -2, *Adv. Immunol. 62*, 167−215.
2. Herschman, H. R. (1996) Prostaglandin synthase 2, *Biochim. Biophys. Acta 1299*, 125−140.
3. Smith, W. L., Eling, T. E., Kulmacz, R. J., Marnett, L. J., and Tsai, A.-L. (1992) Tyrosyl radicals and their role in hydroperoxide-dependent activation and inactivation of prostaglandin endoperoxide synthase, *Biochemistry 31*, 3−7.
4. Lambeir, A. M., Markey, C. M., Dunford, H. B., and Marnett, L. J. (1985) Spectral properties of the higher oxidation states of prostaglandin H synthase, *J. Biol. Chem. 260*, 14894−14896.
5. Dietz, R., Nastainczyk, W., and Ruf, H. H. (1988) Higher oxidation states of prostaglandin H synthase. Rapid electronic spectroscopy detected two spectral intermediates during the peroxidase reaction with prostaglandin G2, *Eur. J. Biochem. 171*, 321−328.
6. Tsai, A.-L., Kulmacz, R. J., and Palmer, G. (1995) Spectroscopic evidence for reaction of prostaglandin H synthase-1 tyrosyl radical with arachidonic acid, *J. Biol. Chem. 270*, 10503−10508.
7. Malkowski, M. G., Ginell, S. L., Smith, W. L., and Garavito, R. M. (2000) The productive conformation of arachidonic acid bound to prostaglandin synthase, *Science 289*, 1933−1937.
8. Tsai, A.-L., and Kulmacz, R. J. (2000) Tyrosyl radicals in prostaglandin H synthase-1 and -2, *Prost. Lipid Med. 62*, 231−254.
9. Tsai, A.-L., Wu, G., Palmer, G., Bambai, B., Koehn, J. A., Marshall, P. J., and Kulmacz, R. J. (1999) Rapid kinetics of tyrosyl radical formation and heme redox state changes in prostaglandin H synthase-1 and -2, *J. Biol. Chem. 274*, 21695−21700.
10. Lassmann, G., Odenwaller, R., Curtis, J. F., DeGray, J. A., Mason, R. P., Marnett, L. J., and Eling, T. E. (1991) Electron spin resonance investigation of tyrosyl radicals of prostaglandin H synthase. Relation to enzyme catalysis, *J. Biol. Chem. 266*, 20045−20055 (erratum: Lassmann, G., Odenwaller, R., Curtis, J. F., DeGray, J. A., Mason, R. P., Marnett, L. J., and Eling, T. E. (1992) *J. Biol. Chem. 267* (9), 6449).
11. Tsai, A.-L., Palmer, G., and Kulmacz, R. J. (1992) Prostaglandin H synthase. Kinetics of tyrosyl radical formation and of cyclooxygenase catalysis, *J. Biol. Chem. 267*, 17753−17759.
12. DeGray, J. A., Lassmann, G., Curtis, J. F., Kennedy, T. A., Marnett, L. J., Eling, T. E., and Mason, R. P. (1992) Spectral analysis of the protein-derived tyrosyl radicals from prostaglandin H synthase, *J. Biol. Chem. 267*, 23583−23588.
13. Kulmacz, R. J., Ren, Y., Tsai, A.-L., and Palmer, G. (1990) Prostaglandin H synthase: spectroscopic studies of the interaction with hydroperoxides and with indomethacin, *Biochemistry 29*, 8760−8771.
14. Xiao, G., Tsai, A.-L., Palmer, G., Boyar, W. C., Marshall, P. J., and Kulmacz, R. J. (1997) Analysis of hydroperoxide-induced tyrosyl radicals and lipoxygenase activity in aspirin-treated human prostaglandin H synthase-2, *Biochemistry 36*, 1836−1845.
15. Shi, W., Hoganson, C. W., Espe, M., Bender, C. J., Babcock, G. T., Palmer, G., Kulmacz, R. J., and Tsai, A.-L. (2000) Electron paramagnetic resonance and electron nuclear double resonance spectroscopic identification and characterization of the tyrosyl radicals in prostaglandin H synthase-1, *Biochemistry 39*, 4112−4121.
16. Dorlet, P., Seibold, S. A., Babcock, G. T., Gerfen, G. J., Smith, W. L., Tsai, A.-L., and Un, S. (2002) High-field EPR study of tyrosyl radicals in prostaglandin H(2) synthase-1, *Biochemistry 41*, 6107−6114.
17. Tsai, A.-L., Hsi, L. C., Kulmacz, R. J., Palmer, G., and Smith, W. L. (1994) Characterization of the tyrosyl radicals in ovine prostaglandin H synthase-1 by isotope replacement and site-directed mutagenesis, *J. Biol. Chem. 269*, 5085−5091.
18. Tsai, A.-L., Palmer, G., Xiao, G., Swinney, D. C., and Kulmacz, R. J. (1998) Structural characterization of arachidonyl radicals

formed by prostaglandin H synthase-2 and prostaglandin H synthase-1 reconstituted with mangano protoporphyrin IX, *J. Biol. Chem. 273*, 3888−3894.
19. Barry, B. A., el-Deeb, M. K., Sandusky, P. O., and Babcock, G. T. (1990) Tyrosine radicals in photosystem II and related model compounds. Characterization by isotopic labeling and EPR spectroscopy, *J. Biol. Chem. 265*, 20139−20143.
20. Onuchic, J. N., Beratan, D. N., Winkler, J. R., and Gray, H. B. (1992) Pathway analysis of protein electron-transfer reactions, *Annu. Rev. Biophys. Biomol. Struct. 21*, 349−377.
21. Beratan, D. N., and Onuchic, J. N. (1996) The protein bridge between redox centers, in *Protein Electron Transfer* (Bendall, D. S., Ed.) pp 23−41, BIOS Science Publishers Ltd., Oxford.
22. Kurumbail, R. G., Stevens, A. M., Gierse, J. K., McDonald, J. J., Stegeman, R. A., Pak, J. Y., Gildehaus, D., Miyashiro, J. M., Penning, T. D., Seibert, K., Isakson, P. C., and Stallings, W. C. (1996) Structural basis for selective inhibition of cyclooxygenase-2 by anti-inflammatory agents, *Nature 384*, 644−648.
23. Guo, Q., Wang, L. H., Ruan, K. H., and Kulmacz, R. J. (1996) Role of Val509 in time-dependent inhibition of human prostaglandin H synthase-2 cyclooxygenase activity by isoform-selective agents, *J. Biol. Chem. 271*, 19134−19139.
24. Bambai, B., Rogge, C. E., Stec, B., and Kulmacz, R. J. (2004) Role of Asn382 and Thr383 in activation and inactivation of human prostaglandin H synthase cyclooxygenase catalysis, *J. Biol. Chem.* (manuscript in press).
25. Kulmacz, R. J., and Lands, W. (1987) Cyclo-oxygenase: measurement, purification and properties in *Prostaglandins and Related Substances: A Practical Approach* (McDonald-Gibson, R. G., Nigam, S., and Slater, T. F., Eds.) pp. 209−227 IRL Press, Washington, DC.
26. Smith, W. L., and Lands, W. E. (1972) Oxygenation of unsaturated fatty acids by soybean lipoxygenase, *J. Biol. Chem. 247*, 1038−1047.
27. Tsai, A.-L., Berka, V., Kulmacz, R. J., Wu, G., and Palmer, G. (1998) An improved sample packing device for rapid freeze-trap electron paramagnetic resonance spectroscopy kinetic measurements, *Anal. Biochem. 264*, 165−171.
28. Kulmacz, R. J. (1986) Prostaglandin H synthase and hydroperoxides: peroxidase reaction and inactivation kinetics, *Arch. Biochem. Biophys. 249*, 273−285.
29. Hsi, L. C., Hoganson, C. W., Babcock, G. T., and Smith, W. L. (1994) Characterization of a tyrosyl radical in prostaglandin endoperoxide synthase-2, *Biochem. Biophys. Res. Commun. 202*, 1592−1598.
30. Tsai, A.-L., Palmer, G., Wu, G., Peng, S., Okeley, N. M., van der Donk, W. A., and Kulmacz, R. J. (2002) Structural characterization of arachidonyl radicals formed by aspirin-treated prostaglandin H synthase-2, *J. Biol. Chem. 277*, 38311−38321.
31. Sjoberg, B. M., Reichard, P., Graslund, A., and Ehrenberg, A. (1978) The tyrosine free-radical in ribonucleotide reductase from Escherichia-coli, *J. Biol. Chem. 253*, 6863−6865.
32. Ivancich, A., Jouve, H. M., Sartor, B., and Gaillard, J. (1997) EPR investigation of compound I in Proteus mirabilis and bovine liver catalases: Formation of porphyrin and tyrosyl radical intermediates, *Biochemistry 36*, 9356−9364.
33. Debus, R. J., Barry, B. A., Sithole, I., Babcock, G. T., and McIntosh, L. (1988) Directed mutagenesis indicates that the donor to P-680+ in photosystem-II Is tyrosine-161 of the D1 polypeptide, *Biochemistry 27*, 9071−9074.
34. Debus, R. J., Barry, B. A., Babcock, G. T., and McIntosh, L. (1988) Site-directed mutagenesis identifies a tyrosine radical involved in the photosynthetic oxygen-evolving system. *Proc. Natl. Acad. Sci. U.S.A. 85*, 427−30.
35. Rogers, M. S., and Dooley, D. M. (2003) Copper-tyrosyl radical enzymes, *Curr. Opin. Chem. Biol. 7*, 189−196.
36. Chouchane, S., Girotto, S., Yu, S., and Magliozzo, R. S. (2002) Identification and characterization of tyrosyl radical formation in Mycobacterium tuberculosis catalase-peroxidase (KatG), *J. Biol. Chem. 277*, 42633−42638.
37. Ryle, M. J., Liu, A., Muthukumaran, R. B., Ho, R. Y. N., Koehntop, K. D., McCracken, J., Que, L. Jr., and Hausinger, R. P. (2003) O2- and alpha-ketoglutarate-dependent tyrosyl radical formation in TauD, an alpha-keto acid-dependent non-heme iron dioxygenase, *Biochemistry 42*, 1854−1862.
38. Svistunenko, D. A., Dunne, J., Fryer, M., Nicholls, P., Reeder, B. J., Wilson, M. T., Bigotti, M. G., Cutruzzola, F., and Cooper, C. E. (2002) Comparative study of tyrosine radicals in hemoglobin and myoglobins treated with hydrogen peroxide, *Biophys. J. 83*, 2845−2855.
39. Seibold, S. A., Cerda, J. F., Mulichak, A. M., Song, I., Garavito, R. M., Arakawa, T., Smith, W. L., and Babcock, G. T. (2000) Peroxidase activity in prostaglandin endoperoxide H synthase-1 occurs with a neutral histidine proximal heme ligand, *Biochemistry 39*, 6616−6624.
40. Kozak, K. R., Prusakiewicz, J. J., Rowlinson, S. W., Schneider, C., and Marnett, L. J. (2001) Amino acid determinants in cyclooxygenase-2 oxygenation of the endocannabinoid 2-arachidonylglycerol, *J. Biol. Chem. 276*, 30072−30077.
41. Rowlinson, S. W., Kiefer, J. R., Prusakiewicz, J. J., Pawlitz, J. L., Kozak, K. R., Kalgutkar, A. S., Stallings, W. C., Kurumbail, R. G., and Marnett, L. J. (2003) A novel mechanism of cyclooxygenase-2 inhibition involving interactions with Ser-530 and Tyr-385. *J. Biol. Chem. 278*, 45763−45769.
42. Smith, W. L., and Lands, W. E. Y. (1972) Oxygenation of polyunsaturated fatty acids during prostaglandin biosynthesis by sheep vesicular gland, *Biochemistry 11*, 3276−3285.
43. Barnett, J., Chow, J., Ives, D., Chiou, M., MacKenzie, R., Osen, E., Nguyen, B., Tsing, S., Bach, C., Freire, J., Chan, H., Sigal, E., and Ramesha, C. (1994) Purification, characterization and selective inhibition of human prostraglandin G/H synthase 1 and 2 expressed in the baculovirus system, *Biochim. Biophys. Acta 1209*, 130−139.
44. Wu, G., Wei, C., Kulmacz, R. J., Osawa, Y., and Tsai, A.-L. (1999) A mechanistic study of self-inactivation of the peroxidase activity in prostaglandin H synthase-1, *J. Biol. Chem. 274*, 9231−9237.
45. Stubbe, J. (1990) Ribonucleotide Reductases: Amazing and Confusing, *J. Biol. Chem. 265*, 5329−5332.
46. Nordlund, P., and Eklund, H. (1993) Structure and Function of the Escherichia coli ribonucleotide reductase protein R2, *J. Mol. Biol. 232*, 123−164.
47. Uhlin, U., and Eklund, H. (1994) The structure of ribonucleotide reductase R1, *Nature 370*, 533−539.
48. Licht, S., Gerfen, G. J., and Stubbe, J. (1996) Thiyl Radicals in Ribonucleotide Reductases, *Science 271*, 477−481.
49. Tommos, C., Hoganson, C. W., Valentin, M. D., Lydakis-Simantiris, N., Dorlet, P., Westphal, K., Chu, H. A., McCracken, J., and Babcock, G. T. (1998) Manganese and tyrosyl radical function in photosynthetic oxygen evolution, *Curr. Opin. Chem. Biol. 2*, 244−252.

BI035717O